

C–S Bond Activation and Partial Hydrogenation of Thiophene by a Dinuclear Trihydride Platinum Complex

Ainara Nova,^[a] Fernando Novio,^[a] Pilar González-Duarte,^{*[a]} Agustí Lledós,^{*[a]} and Rubén Mas-Ballesté^[a]

Keywords: C–S activation / Desulfurization / Thiophene / Hydride ligands / Platinum / Reaction mechanisms

[(dppp)₂Pt₂H₃]ClO₄ [**I**, dppp = Ph₂P(CH₂)₃PPh₂] was found to activate the C–S bond and to cause partial hydrogenation of thiophene. Thus, the reaction of **I** with neat thiophene (**T**) at reflux temperature yields [(dppp)Pt(SC₄H₄-C,S)] (**II**) and [(dppp)₂Pt₂(μ-SC₄H₅-C,S)]ClO₄ (**III**) at a 2:3 molar ratio. The same reaction in toluene or benzene solvent affords the same complexes **II** and **III** but in a 1:9 molar ratio. The concomitant formation of **II** and **III** was interpreted on the basis of theoretical calculations (DFT), which have provided a detailed insight into the reaction mechanism. Thus, the presence of **T** causes **I** to dissociate into [(dppp)PtH₂] and [(dppp)PtH(C₄H₄S-κS)], this process being a common step for the two ensuing reaction pathways. After dissociation, the activation of the thiophene C–S bond to yield **II** involves participation of [(dppp)PtH₂] exclusively. However, the reaction leading to **III** requires the internal migration of the coordi-

nated hydride to the thiophene ligand in [(dppp)PtH(C₄H₄S-κS)] and the subsequent assistance of the {(dppp)Pt} fragment formed from [(dppp)PtH₂] by hydrogen elimination. As a result of the involvement of [(dppp)PtH₂] in the formation of both **II** and **III**, the two reaction pathways are competitive. The reactivity of **II** and **III** with various sources of hydride ligands and different protonic acids has also been examined. Thus, the reaction of **II** with HBF₄ leads to the thiolate-bridged dinuclear complex [(dppp)₂Pt₂(μ-SC₄H₅)₂](BF₄)₂ (**IV**). In the case of **III** the addition of HBF₄ leads to [(dppp)₂Pt₂(μ-SC₄H₆)](BF₄)₂ (**V**), which transforms into **III** by the addition of a base. The X-ray structural characterization of the unprecedented complex **V** is reported here.

(© Wiley-VCH Verlag GmbH & Co. KGaA, 69451 Weinheim, Germany, 2007)

Introduction

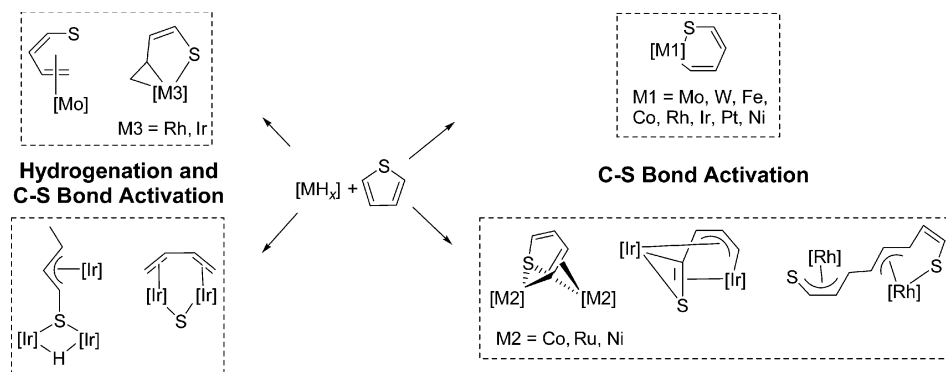
The reaction of thiophenes with homogeneous transition metals is considered a good strategy for modeling heterogeneous reactions that occur during the hydrodesulfurization (HDS) of petroleum.^[1–6] This is a step in industrial oil refining in which sulfur is removed from crude oil by being chemically converted to H₂S and hydrocarbon products.^[7,8] Conventionally, the HDS process involves a reaction with hydrogen gas (up to 200 atm pressure) at temperatures of 300–450 °C over an alumina supported cobalt (or nickel) molybdenum catalyst. The evident importance of HDS together with environmental regulations that dictate increasingly smaller amounts of sulfur in gasoline and gasoil fuels^[9,10] account for the current interest in developing more efficient technologies. Several reviews of the results obtained in the search for new heterogeneous catalysts,^[11–15] in homogeneous modeling studies with transition-metal complexes^[1,2,4,16–18] and in computational stud-

ies dealing with several aspects of heterogeneous HDS,^[19–23] have already appeared. Remarkably, despite the large number of studies, the mechanism for the heterogeneous HDS of thiophenic molecules is not completely known and current technology has been unsuccessful in treating these compounds to achieve the sulfur levels required by new legislation.

The reactions of thiophenes with soluble metal complexes have provided mechanistic knowledge of the HDS process.^[1,5,24–26] Significantly, many metals (Ru, Os, Ir, Re, Pt, Pd) have been shown to be more active as HDS promoters than the molybdenum–cobalt (or nickel) mixtures usually employed in industrial HDS.^[10,12–14,27–30] Thus, the reaction of thiophene (**T**) with mono- or dinuclear transition-metal complexes has usually led to the cleavage of a single thiophene C–S bond and thus to the formation of a thiametalacycle as the product^[4,31–41] (Scheme 1, right-hand side). Concerning these reactions, the most thorough mechanistic study involves a mononuclear rhodium species.^[34] Although no intermediates were detected in this reaction, the use of selectively deuterated reagents and theoretical calculations made it possible to propose the corresponding mechanism.^[42–44] In terms of mono- and dinuclear transition-metal complexes, the only example of a complete desulfurization of thiophene to butadiene was achieved by

[a] Departament de Química, Universitat Autònoma de Barcelona, 08193 Bellaterra, Barcelona, Spain
Fax: +34-935813101
E-mail: Pilar.Gonzalez.Duarte@uab.es
agusti@klingon.uab.es

Supporting information for this article is available on the WWW under <http://www.eurjic.org> or from the author.



Scheme 1. Reported products obtained in the reaction of **T** with [MH_x] ($x = 0-3$) transition-metal complexes.

means of a dinuclear polyhydride iridium complex in the presence of a hydrogen acceptor compound.^[45] Several intermediate species identified by NMR showed how the activation of the second C–S bond is subsequent to the hydrogenation of the thiophenic chain. Within this context, it is worth noting that in the examples where the first C–S bond activation is accompanied by hydrogenation (Scheme 1, left-hand side),^[32,46,47] the complete desulfurization has usually required further treatment with H₂. However, the same reaction with the thiametalacycle products is unreported.

In this paper, a dinuclear polyhydride platinum complex was investigated for its ability to react with **T**. An approach followed in earlier studies of platinum-mediated desulfurization of thiophene, benzothiophene, and dibenzothiophene involved their reaction with [(PEt₃)₃Pt] and subsequent treatment with various hydride reagents.^[35] While the completely desulfurized hydrocarbons were obtained from the three heterocycles, the amount of desulfurization in the case of **T** was about 4%. Overall, the notion that two metal centers might be required for cleavage of both thiophenic C–S bonds,^[16] the high HDS activity shown by platinum metals,^[48,49] and the fact that a polyhydride complex already contains the hydrogen needed for thiophene hydrogenolysis led us to explore the reaction of [(dppp)₂Pt₂H₃]-ClO₄ [dppp = 1,3-bis(diphenylphosphanyl)propane] with **T** and the mechanism of this reaction. Within the context of its possible relevance in the modeling of HDS studies, we first investigated the reactivity of [(dppp)₂Pt₂H₃]-ClO₄ toward sulfur-containing species such as Na₂S or NaSH. The set of reactions obtained provided solid evidence that behind the apparent simplicity of platinum complexes containing Pt–H, Pt–SH, or Pt–S fragments, there is an outstanding chemistry.^[50]

Results and Discussion

Experimental Results

The reaction between [(dppp)₂Pt₂H₃]-ClO₄ (**I**) and **T** was monitored by ¹H and ³¹P NMR and mass measurements until no further progress was observed. Consistent with literature data,^[35,36,45] high temperature, significant excess of thiophene with respect to the platinum complex, and sev-

eral hours are required for optimum rate and yield. While under these experimental conditions we always observed the concomitant formation of two platinum complexes, their relative amounts were dependent on the presence or absence of benzene or toluene solvent. The isolation procedure and complete characterization of the complexes obtained are given in the Experimental Section.

The Reaction of [(dppp)₂Pt₂H₃]-ClO₄ (**I**) with Thiophene

Monitoring by ³¹P NMR spectroscopy (Figure 1) indicated concomitant formation of a mononuclear and a dinuclear platinum species (Scheme 2). However, neither the NMR nor the ESI MS data gave evidence of intermediate species being formed. Similar observations were obtained in the monitoring of the reaction of **I** (0.15 mmol) with thiophene (15 mL) in toluene or benzene solvent (15–20 mL) at reflux temperature. The only difference in these reactions was the relative molar ratio of the two new platinum complexes formed (2:3 in neat thiophene and 1:9 in toluene or benzene). According to the ³¹P and ¹H NMR spectroscopic data recorded during the reaction, both **II** and **III** not only form simultaneously but also maintain a constant molar ratio until the end of the reaction.

The ³¹P NMR features of the reaction mixture that were attributable to a mononuclear platinum complex, literature data,^[35,36] and the peak at $m/z = 692.2$ in the ESI MS spectrum were consistent with the formation of an unsymmetrical species by insertion of the {(dppp)Pt} fragment into one thiophenic C–S bond. The formulation of this complex as [(dppp)Pt(SC₄H₄-C,S)] (**II**) was fully confirmed by ³¹P, ¹⁹⁵Pt{¹H} and bidimensional ¹H and ¹³C spectra (NOESY, COSY, HMQC C-H, and HSQC-edit C-H). ¹H and ¹³C NMR spectroscopic data were consistent with those reported for the related [(PEt₃)₂Pt(SC₄H₄-C,S)] complex.^[35]

The remaining signals in the ³¹P NMR spectrum of the reaction mixture, together with ¹H NMR and ESI MS data obtained during the monitoring of the reaction of **I** with **T** gave evidence that **III** was probably a dinuclear platinum complex. Full characterization of this complex after its isolation by column chromatography from crude mixture after 20 h of reaction allowed us to formulate it as [(dppp)₂Pt₂(μ-SC₄H₅-C,S)]ClO₄ (**III**).

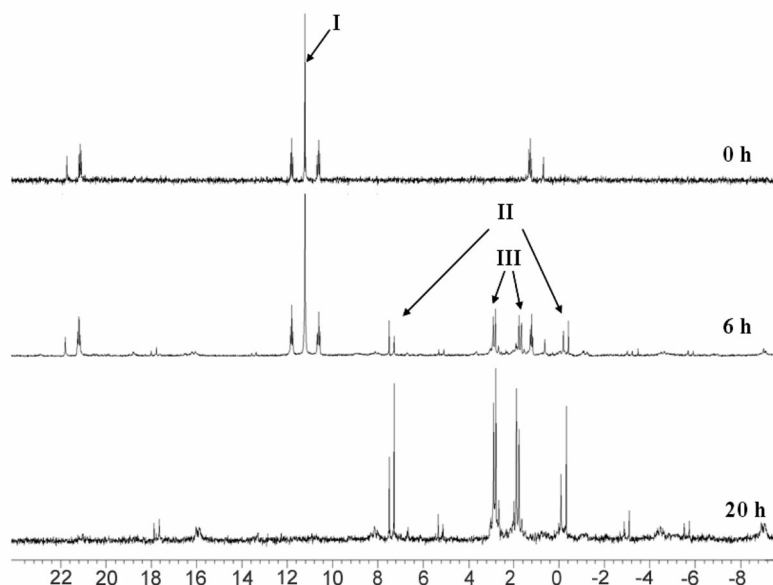
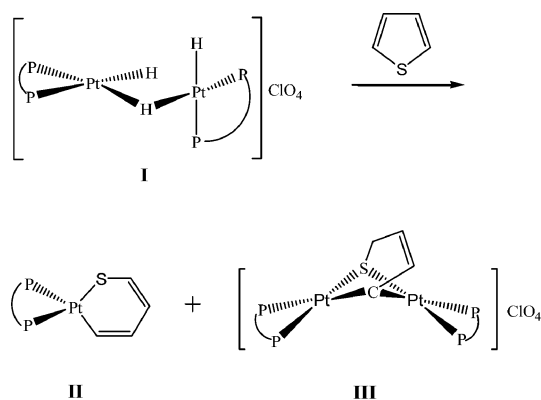


Figure 1. Monitoring by $^{31}\text{P}\{^1\text{H}\}$ NMR in Cl_3CD of the reaction of $[(\text{dppp})_2\text{Pt}_2\text{H}_3]\text{ClO}_4$ (**I**) with neat thiophene evidences formation of $[(\text{dppp})\text{Pt}(\text{SC}_4\text{H}_4\text{-C,S})]$ (**II**) and $[(\text{dppp})_2\text{Pt}_2(\mu\text{-SC}_4\text{H}_5\text{-C,S})]\text{ClO}_4$ (**III**) after 6 h, and total consumption of **I** after 20 h.



Scheme 2. The mono- and dinuclear platinum complexes obtained in the reaction of **I** with thiophene.

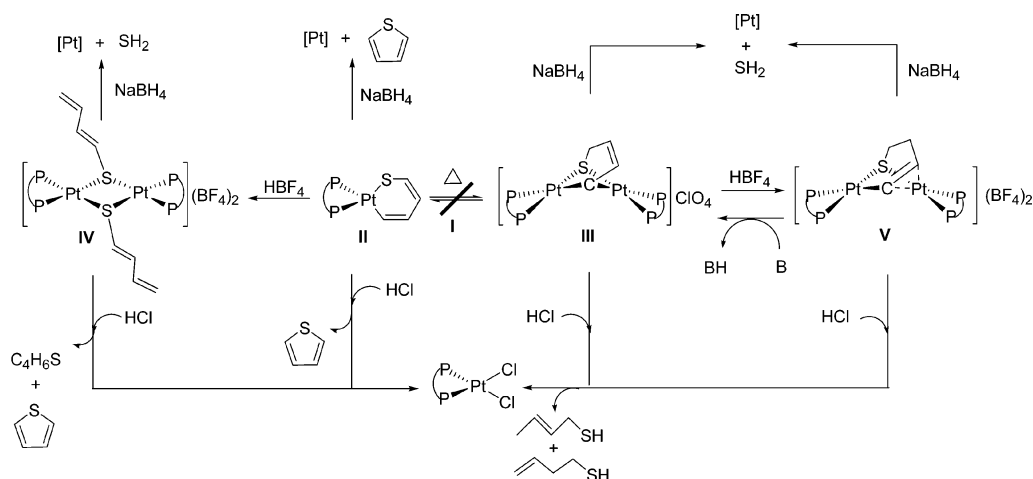
Thus, the $^{31}\text{P}\{^1\text{H}\}$ NMR spectrum of **III** is second-order, consisting of two broad signals (Figure 1) that fit well with the simulation of this spectrum including long-range P–Pt couplings (see electronic supporting information). Concerning the $^{195}\text{Pt}\{^1\text{H}\}$ NMR spectrum, it displays the same pattern as **II** with broader signals. These features corroborate the dinuclear nature of **III** and the symmetrical behavior of the bridging ligand. The SC_4H_5 ligand in **III** was fully characterized by ^1H NMR, with additional NOESY and COSY experiments, as well as by HMBC P–H, ^{13}C NMR (DEPT), and HSQC-edit C–H data. The ^{13}C chemical shifts at $\delta = 126.1$ and 137.1 ppm, which are in the proper range for olefins, gave evidence of one double bond. This fact, in addition to the symmetry of the complex, even at low temperatures, allows an η^3 coordination for this bridge to be discarded and makes the formulation $\{\text{S}-\text{CH}_2-\text{CH}=\text{CH}-\text{CH}\}$ the most reasonable alternative.^[51] The stoichiometric ratio of dppp to SC_4H_5 ligands in **III** is 2:1, as deduced from the integration of the signals of the proton

resonating at $\delta = 5.43$ or 5.61 ppm (corresponding to the $-\text{CH}=\text{CH}-$ fragment) with respect to those of the aliphatic CH_2 groups in the phosphane ligands, in agreement with the dinuclear nature of **III**. The absence of hydride ligands is fully confirmed by ^1H and HMBC Pt–H NMR, and agrees with infrared data. Finally, the ESI-MS spectrum shows a major peak at $m/z = 1299.2401$ [M^+] that fits well to the $[(\text{dppp})_2\text{Pt}_2(\text{SC}_4\text{H}_5)]^+$ cation. Elemental analyses and IR data are consistent with **III** being an ionic molecule with ClO_4^- as counterion.

Additional Reactions

In order to further elucidate the mechanism leading to **II** and **III**, and to further analyze the reactivity of these complexes, we carried out complementary reactions. These were monitored for several hours by ^{31}P and ^1H NMR as earlier described for the reaction of **I** with **T**. In some reactions the deuterated analog of **I**, $[(\text{dppp})_2\text{Pt}_2\text{D}_3]\text{ClO}_4$ (**I-d₃**), was employed, and in these cases ^2H NMR spectra were also recorded. The synthesis and NMR features of **I-d₃** have already been reported.^[50] On the whole the NMR features allowed identification of the compounds formed and eventually led to the synthesis and characterization of new complexes, as depicted in Scheme 3.

The reactions involving **I-d₃** gave evidence that complex **I** cleaves in the presence of thiophene. Thus, the heating at reflux temperature of a 1:1 mixture of **I** and **I-d₃** in the presence of thiophene showed that after 6 h all isotopomers $[(\text{dppp})_2\text{Pt}_2\text{H}_{(3-x)}\text{D}_x]^+$ ($x = 0-3$) were present in comparable amounts. However, when the same process was carried out in the absence of thiophene, only negligible amounts of mixed species were present after 12 h of heating. This indicated that **T**, and not the presence of solvent, causes the cleavage of **I**, and that the breaking of the dinuclear platinum complex **I** is a reversible process, both issues being



Scheme 3. Overall reactivity of complexes I–V: (a) No interconversion between II and III is observed; (b) II with HBF₄ affords IV and, similarly, III gives V; (c) V goes back to III by addition of a base (B = MeO[−], Et₃N); (d) complexes II–V react with HCl, and also with NaBH₄, but not with I.

consistent with literature data.^[32] In addition to the above reactions, the use of **I-d₃** provided information on the source and location of the inserted hydrogen atom into the thiophenic chain of **III**. This was obtained by the reaction of **I-d₃** and **T** in toluene at reflux temperature, which afforded **II** and **III-d₁**. Characterization of **III-d₁** by ¹H, ²H, and ¹³C DEPT-135 NMR spectroscopic data allows to establish that deuterium is bound to the carbon atom next to the sulfur atom.

Another set of experiments, aimed at examining whether **II** and **III** could convert into each other even though their concentrations increased concomitantly during the reaction of **I** with **T**, both in the presence and absence of toluene or benzene solvent, was indicative of parallel reaction pathways. Within this context, **II** and **III** were independently heated in toluene solvent at reflux temperature for several hours, during which no changes were observed. The same procedure with a mixture of **I** (as a possible platinum and hydride source) and **II** at various molar ratios in toluene did not afford **III**, thus reinforcing that **II** and **III** are independently formed.

While the reaction of **I** with **T** involves the activation of one C–S bond of thiophene, the conditions for the cleavage of the second S–C bond in **II** and **III** were also examined. To this end, complexes **II** and **III** were made to react with protonic acids (HBF₄, HCl) and hydride sources (NaBH₄, **I**). These reactions are summarized in Scheme 3 and the corresponding conditions given in the Exp. Section.

The Reaction of II and III with HBF₄

The reaction of **II** with HBF₄ yielded the di-μ-thiolato dinuclear complex [(dppp)₂Pt₂(μ-SC₄H₅)₂](BF₄)₂ (**IV**) in high yield. Identification of this complex was achieved on the basis of NMR spectroscopic data, which were fully consistent with those reported for the [(PEt₃)₄Pt₂(μ-SC₄H₅)₂](BF₄)₂ analog, also obtained in a parallel reaction.^[52]

Remarkably, replacement of **II** by **III** in the above reaction led to the unprecedented complex [(dppp)₂Pt₂(μ-

SC₄H₆)](BF₄)₂ (**V**), whose formation involves the insertion of a proton in the thiophenic chain of **III** without cleavage of the dinuclear species. As shown in Scheme 3, this reaction is easily reversed by addition of a base (NaMeO, NEt₃). Characterization of **V** by solution NMR measurements at room temperature evidenced the symmetrical behavior of the bridging ligand with respect to the two platinum centers. It also allows to establish that the proton insertion in the bridging S–CH₂–CH=CH–CH ligand in **III** causes an electronic rearrangement leading to a S–CH₂–CH₂–CH=CH species in **V**. As a result, one of the two σ Pt–C5 bonds in **III** evolved into a π interaction with the C4=C5 double bond in **V**, consistently with ¹H and ¹³C NMR spectroscopic data. However, the symmetry observed in the latter complex for the phosphorus nuclei in the ³¹P{¹H} NMR spectrum indicated a fluxional behavior for the CH=CH ligand moiety, which was consistent with low-temperature ³¹P{¹H} NMR spectroscopic data. These showed that the two signals corresponding to the phosphorus nuclei, particularly that at δ = 0.1 ppm, widen with decreasing temperature without reaching complete decoalescence. According to the structure determined by single-crystal X-ray diffraction (see below), the features above are consistent with a fluxional behavior for the bridging ligand, which involves the σ Pt–C5 bond and the C4=C5 double bond to exchange sites between the two platinum centers.

The Reaction of II–V with HCl

The reaction of **II–V** with a slight excess of HCl always led to the separation of solid [(dppp)PtCl₂] in high yield (about 75%). The ease of formation of this complex in related systems is well known.^[52] In the case of **III–V**, various thiols were also detected in the reaction mixture by CG-MS, as depicted in Scheme 3. Thiophene was also identified in the reaction of **IV**, and it was the only additional product in the case of **II**, both results being consistent with reported data.^[52]

Overall, the reaction of **II–V** with HBF_4 or HCl does not involve activation of the second thiophenic C–S bond. Instead, these reactions allow the formation of thiols and, in the case of HCl , the recovery of platinum as $[(\text{dppp})\text{PtCl}_2]$.

The Reaction of **II–V** with **I** and NaBH_4

Complexes **II–V** did not react with **I** in toluene at reflux temperature but started degrading after 12 h of heating, as evidenced by the darkening of the reaction mixture, which was attributed to the formation of Pt^0 . The same features were observed in the attempts to treat **II–V** with NaBH_4 at room temperature. However, with NaBH_4 the darkening of the solution was accompanied by the formation of either **T** (**II**) or H_2S (**III–V**), the former detected by GC-MS, and the latter by formation of silver sulfide. Significantly, no other sulfur-containing species were identified in these reactions.

On the basis of the reactions above, it becomes apparent that the activation of the second thiophenic S–C bond by hydride sources is only achieved in compounds **III–V**. The reluctance of this bond to be activated in **II** is probably due to the greater aromatic character of the corresponding thiametalacycle. In fact, the cleavage of the C–S bond in **II** requires previous treatment with protons in the presence of noncoordinating counterions (HBF_4), which leads to **IV**. Overall, the activation of the C–S bond in **II–V** by NaBH_4 involves the total decomposition of these complexes.

X-ray Structure of the $[(\text{dppp})\text{Pt}(\mu\text{-SC}_4\text{H}_6)\text{Pt}(\text{dppp})]^{2+}$ Cation

The structure showed evidence of a twinned crystal having two components related by a twofold rotation along the reciprocal axis c^* . The asymmetric unit of the unit cell contains two cations $[(\text{dppp})\text{Pt}(\mu\text{-SC}_4\text{H}_6)\text{Pt}(\text{dppp})]^{2+}$ together with three BF_4^- and one ClO_4^- anions, three acetone and one water molecules.^[53] As the bonding parameters of the two cations are comparable, the geometry and selected bond lengths and angles given in the text correspond to one of them (Figure 2, Tables 1 and 2).

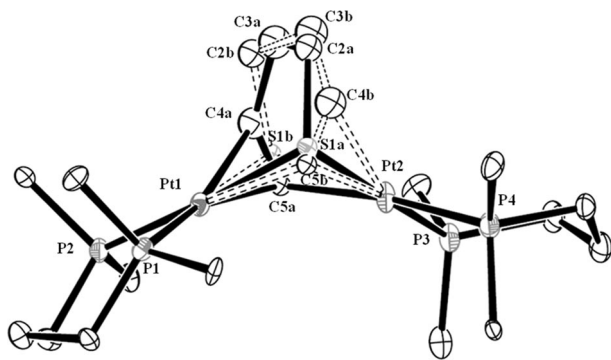


Figure 2. Structure of the cation in complex **V** with 50% probability displacement ellipsoids showing the two opposite orientations (a/b) of the thiolate bridge. Anions, hydrogen atoms, and phenyl rings are omitted for clarity.

Table 1. Selected distances [Å] for the cation of complex **V**.

Distances ^[a]			
Pt1–S1A	2.339(4)	Pt2–S1B	2.343(6)
Pt2–S1A	2.357(4)	Pt1–S1B	2.391(6)
Pt1–C5A	2.255(12)	Pt2–C5B	2.30(2)
Pt2–C5A	2.119(12)	Pt1–C5B	2.23(2)
Pt1–C4A	2.376(15)	Pt2–C4B	2.38(2)
S1A–C2A	1.789(11)	S1B–C2B	1.786(13)
C2A–C3A	1.569(14)	C2B–C3B	1.572(15)
C3A–C4A	1.616(14)	C3B–C4B	1.618(15)
C4A–C5A	1.131(14)	C4B–C5B	1.131(15)
Pt1–P1	2.273(2)	Pt2–P3	2.261(2)
Pt1–P2	2.284(2)	Pt2–P4	2.281(2)
Pt1–Pt2	3.2272(6)		

[a] The A/B labels refer to the two disordered SC_4H_6 fragments.

Table 2. Selected angles [°] for the cation of complex **V**.

Angles ^[a]			
Pt1–Pt2–S1A	46.36(10)	Pt2–Pt1–S1B	47.64(16)
Pt2–Pt1–S1A	46.83(11)	Pt1–Pt2–S1B	46.41(15)
Pt1–Pt2–C5A	44.1(3)	Pt2–Pt1–C5B	45.4(6)
Pt2–Pt1–C5A	40.8(3)	Pt1–Pt2–C5B	43.8(6)
Pt1–S1A–Pt2	86.81(13)	Pt2–S1B–Pt1	85.9(2)
Pt1–C5A–Pt2	95.0(5)	Pt2–C5B–Pt1	90.8(7)
S1A–Pt1–C5A	80.5(3)	S1B–Pt2–C5B	80.4(5)
S1A–Pt1–C4A	79.1(3)	S1B–Pt2–C4B	77.4(4)
S1A–Pt2–C5A	82.9(3)	S1B–Pt1–C5B	82.8(5)
S1A–C2A–C3A	113.4(8)	S1B–C2B–C3B	110.4(10)
C2A–C3A–C4A	115.2(10)	C2B–C3B–C4B	116.0(12)
C3A–C4A–C5A	137.3(12)	C3B–C4B–C5B	141.2(16)
Pt1–S1A–C2A	102.9(5)	Pt2–S1B–C2B	104.8(7)
Pt2–S1A–C2A	92.7(6)	Pt1–S1B–C2B	90.7(10)
Pt1–C5A–C4A	81.9(9)	Pt2–C5B–C4B	80.0(16)
Pt2–C5A–C4A	115.0(10)	Pt1–C5B–C4B	114.5(14)
P1–Pt1–S1A	94.37(11)	P3–Pt2–S1B	94.64(16)
P4–Pt2–S1A	94.34(11)	P2–Pt1–S1B	94.29(16)
P2–Pt1–C5A	93.8(3)	P4–Pt2–C5B	92.4(6)
P3–Pt2–C5A	90.1(3)	P1–Pt1–C5B	90.7(5)
P1–Pt1–C5A	164.4(3)	P4–Pt2–S1B	171.63(17)
P2–Pt1–S1A	173.08(11)	P1–Pt1–S1B	173.54(16)
P3–Pt2–S1A	172.45(11)	P3–Pt2–C5B	171.9(5)
P4–Pt2–C5A	171.4(4)	P2–Pt1–C5B	174.6(7)
C5A–Pt1–C4A	28.1(4)	C5B–Pt2–C4B	27.9(4)
P1–Pt1–P2	92.13(8)	P3–Pt2–P4	92.99(8)
P1–Pt1–Pt2	126.72(6)	P3–Pt2–Pt1	128.55(6)
P2–Pt1–Pt2	129.58(6)	P4–Pt2–Pt1	129.30(6)

[a] The A/B labels refer to the two disordered SC_4H_6 fragments.

While the solution of the structure of the cation showed evidence of disorder of the bridging SC_4H_6 ligand, on the basis of the NMR spectroscopic data already described it was modeled as $\text{S-CH}_2\text{-CH}_2\text{-CH=CH}$. On the other hand, crystallographic resolution of a related cobalt complex^[41] allowed us to consider that there were two bridging ligands with opposite orientation, in which the sulfur and C=C double bond exchange sites and the double bond changes the platinum atom, to which it is η^2 -bound (effectively a C_2 rotation of the SC_4H_6 group perpendicular to Pt–Pt axis). Moreover, there was no evidence for disordered atoms corresponding to $\{(\text{dppp})\text{Pt}\}$ moieties, suggesting that these

atoms lie in virtually the same locations in the disordered partners.

The bond lengths and angles observed for the SC₄H₆ ligand are fully consistent with the sequence S–CH₂–CH₂–CH=CH, whose atoms are puckered in such a fashion so that sulfur, C2, C3, and C4 are nearly planar, but with C5 lying above this plane. While one of the platinum atoms (Pt1) is bound to the SC₄H₆ bridge through sulfur and the C4=C5 double bond, the other platinum (Pt2) binds to the same sulfur but only to C5 through a σ bond. As a result of the different coordinative behavior of the bridging ligand, two different square-planar environments are observed for the platinum centers. The platinum–platinum distance of 3.2272(6) Å is consistent with the only reported related species, where a weak metal–metal interaction is proposed.^[54] Concerning the terminal dppp ligands, they adopt a distorted chair conformation that compares very well with that usually found in dinuclear complexes enclosing different bridging ligands between two {(dppp)Pt^{II}} fragments.^[55] This is the first structurally characterized example of a dinuclear platinum compound resulting from the S–C activation of thiophene.

Computational Study of the Reaction Mechanism of **I** with **T**

Computational chemistry has proven to be a useful tool in mechanistic studies of homogeneous catalytic processes.^[56,57] However, theoretical analyses of HDS mechanisms using organometallic reagents are still scarce,^[43,44] and in general have focused on investigating the nature and energetics of the interactions between **T** and single-metal organometallic complexes.^[58–64] In this section we present a complete computational study of the reaction mechanism of **I** with **T** using DFT methods. From this study and the experimental results presented above we propose a plausible reaction pathway for the formation of complexes **II** and **III**.

All complexes have been modeled using H₂P(CH₂)₂PH₂ (dhpp) instead of the actual dppp ligand. The calculated intermediates are numbered from **1** to **10** and the transition states are labeled as **TS1**, **TS2**, and so forth. The van der Waals complexes are indicated by **2a**⋯**2b** while **2a**+**2b** indicates the sum of the energies of the individual species. Given the cationic nature of some intermediates, the in-

clusion of solvent is mandatory to obtain a reliable energy profile. Thus, the relative energies of intermediates and reaction barriers calculated in benzene are given in the schemes. The resulting ΔG values in benzene and details of geometries of the transition states are given in the electronic supporting information.

Fragmentation of the Dinuclear [(dhpp)₂Pt₂H₃]⁺ Cation (**1**)

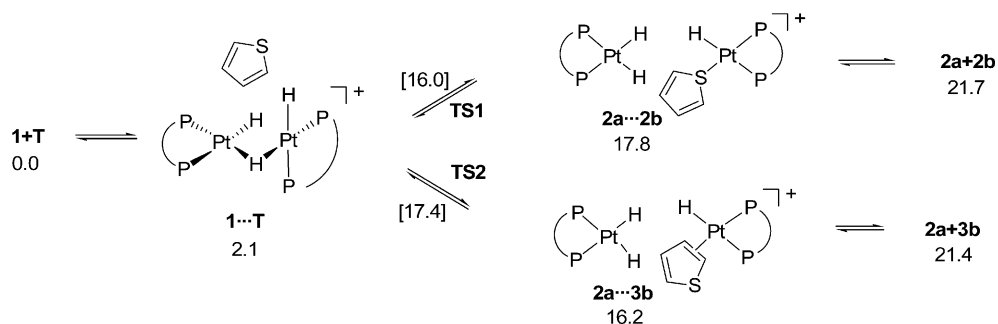
All attempts to make **1** react with **T** have led to the cleavage of the dinuclear platinum complex with the concomitant coordination of **T** to one of the platinum centers. In this way two mononuclear Pt^{II} complexes are formed: [(dhpp)PtH₂] (**2a**) and either [(dhpp)PtH(C₄H₄S- κ S)]⁺ (**2b**) or [(dhpp)PtH(η^2 -C₄H₄S)]⁺ (**3b**), depending on whether the coordination mode of thiophene to platinum is through sulfur or a double bond, respectively. As shown in Scheme 4, both types of coordination involve similar energy barriers: 16.0 kcal/mol (**TS1**) to give **2a** and **2b**; and 17.4 kcal/mol (**TS2**) to give **2a** and **3b**. Also, both pathways are clearly endothermic, the products being 21 kcal/mol above reactants.

The energy for the cleavage of **1** was also calculated in the absence of **T** in order to quantify the thiophene assistance to the fragmentation process. The energy cost associated to the formation of [(dhpp)PtH]⁺ and [(dhpp)PtH₂] (**2a**) from [(dhpp)Pt₂H₃]⁺ in benzene is 39.5 kcal/mol, thus, considerably higher than in the presence of thiophene (21.7 kcal/mol).

Formation of [(dhpp)Pt(C₄H₄S-C,S)] (**6a**)

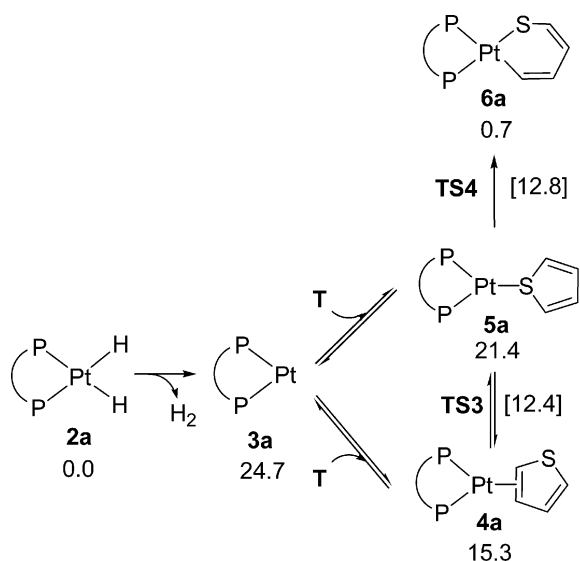
Both **2a** and **2b** species are candidates to afford the {(dhpp)Pt⁰} fragment, which is the precursor of **6a** (**II**). However, theoretical calculations show that formation of this fragment by reductive elimination of H₂ from **2a** is much more easily achieved than the elimination of a *S*-protonated thiophene from **2b**. The calculated energy for the latter reaction is 69.5 kcal/mol, too high to be feasible. Consequently, only the reaction from **2a** to yield **6a** has been taken into account. Concerning energy values, as **2a** and **2b** can exist as separate entities in solution, they are taken as the zero of energy in the following discussions.

The set of reactions that account for the evolution from **2a** to **6a** (Scheme 5) is initiated by the concomitant re-



Scheme 4. Reaction pathway proposed for the fragmentation of **I** (**1**). Relative energies of intermediates and energy barriers (in brackets) are included. All values calculated in benzene solvent [kcal/mol].

duction of platinum and elimination of H₂ (**2a**) to give [(dhpp)Pt] (**3a**), which is 24.7 kcal/mol less stable than **2a**. This is consistent with already reported experimental^[65–67] and theoretical^[68,69] studies. The energy barrier for the H₂ elimination is given by the energy difference between **3a**+H₂ and **2a**. However, as this energy increases monotonously along the H₂ elimination process, the TS cannot be found. This dissociative reaction is entropically favored and, consequently, considering $\Delta G_{\text{benzene}}$ values, **3a**+H₂ lie only 14.5 kcal/mol above **2a**.



Scheme 5. Reaction pathway proposed for the formation of **II** (**6a**). Relative energies of intermediates and energy barriers (in brackets) are included. All values calculated in benzene solvent [kcal/mol].

The next step is the coordination of thiophene to **3a**, which, analogously to the [(dhpp)PtH]⁺ fragment (Scheme 4), can occur through either the sulfur atom or the double bond, thus forming [(dhpp)Pt(C₄H₄S- κ S)] (**5a**) or [(dhpp)Pt(η^2 -C₄H₄S)] (**4a**), respectively. The conversion of **4a** to **5a** is possible through an energy barrier of 12.4 kcal/mol (TS3). In addition, despite **4a** being more stable than **5a** (see Scheme 5), the oxidative addition of platinum to the C–S bond requires that **T** is bound through sulfur. The energy barrier for the oxidative addition process is 12.8 kcal/mol (TS4). Considering the two steps (H₂ elimination + C–

S insertion), TS4 lies 34.2 kcal/mol above **2a**. However, the insertion product [(dhpp)Pt(C₄H₄S-C,S)] (**6a**, Scheme 5) is remarkably stable, as shown by the exothermicity of the insertion process (from **3a** to **6a**).

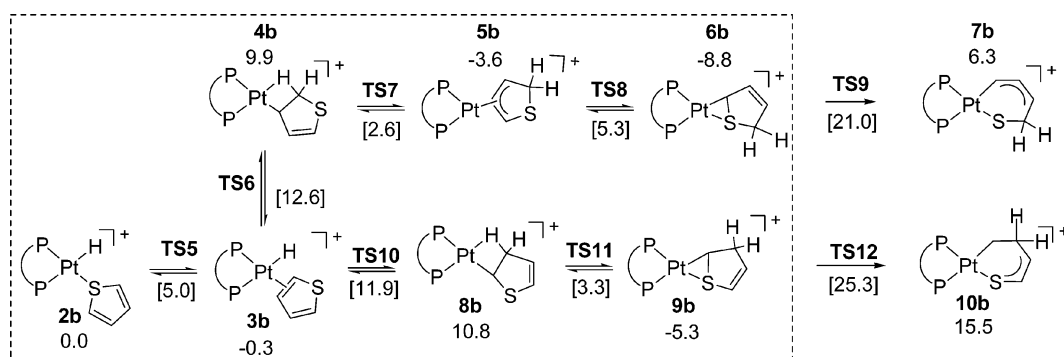
Transfer of Hydride from the Metal to Thiophene

The cationic complex **2b** formed in the first step of the reaction (Scheme 4) follows a different route than **2a**. First, the apparent rotation of thiophene from κ S to η^2 -C,C coordination mode gives way to complex [(dhpp)PtH(η^2 -C₄H₄S)]⁺ (**3b**), with an energy barrier of 5.0 kcal/mol (TS5) (Scheme 6). Complex **3b** can also be formed by direct reaction of **1** with **T** through TS2 (Scheme 4).

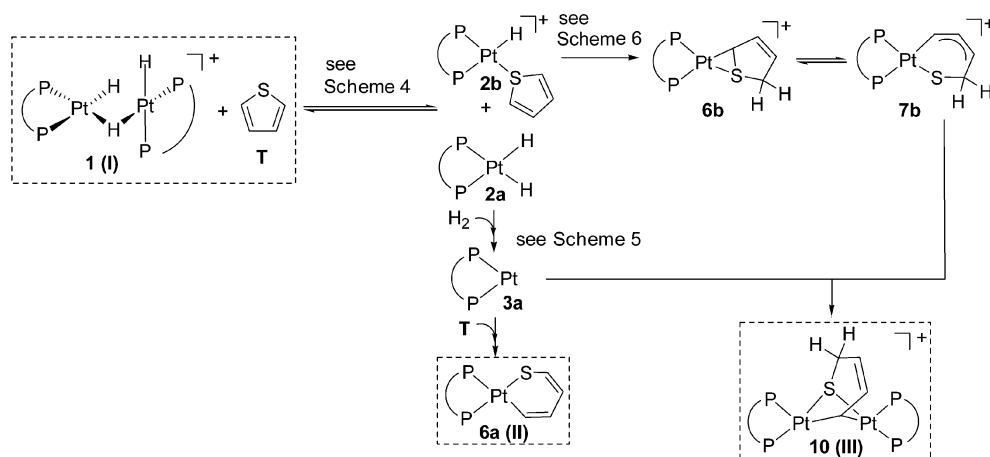
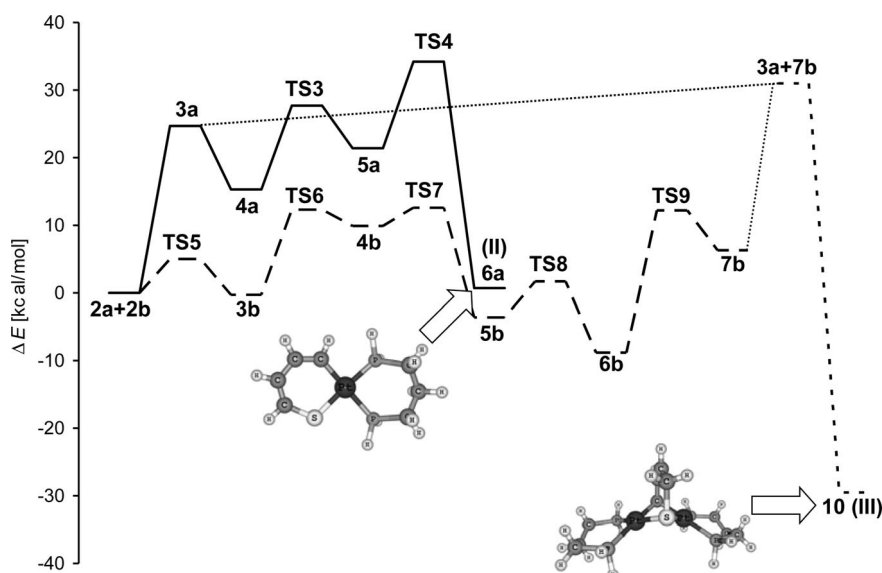
Once **3b** is formed, the hydride migration to the double bond in C2 or C3 becomes feasible. The migration to C2 gives an agostic intermediate **4b** with an energy barrier of 12.6 kcal/mol (TS6). In going from **4b** to **5b** the agostic interaction is lost and the thiophene ring rotates in order to adopt η^3 coordination. The energy cost of this process is very low, only 2.6 kcal/mol (TS7). Finally, from **5b** a subsequent rotation of the thiophene ring with an energy barrier of 5.3 kcal/mol (TS8) gives the most stable conformation of this system (**6b**), 8.8 kcal/mol more stable than **2b**. In **6b** the platinum is bonded to C5 and to the sulfur, and the π system has been rearranged.

From **3b** the hydride migration to C3 proceeds in a similar way, with an energy barrier of 11.9 kcal/mol. After the first transition state (TS10) an agostic intermediate **8b** is formed. The rotation of the thiophenic group in this case gives compound **9b**, where Pt is bonded to the C2 and sulfur atoms. This product is 5.3 kcal/mol more stable than **2b**.

Considering the energy barriers for the hydride transfer and for the thiophene ring rotation, all species displayed in Scheme 6 within the dashed-line square are in equilibrium with each other, although it is displaced towards formation of **6b**. From this complex, the C–S bond activation of thiophene to give complex **7b** is accessible with an energy barrier of 21.0 kcal/mol. The C–S bond activation from the less stable complex **9b** was also considered. This activation not only has a higher energy barrier (25.3 kcal/mol), but also it is a more endothermic reaction. Thus, while **7b** is 6.3 kcal/mol above **2b**, **10b** is 15.5 kcal/mol, so the activated product **7b** is clearly favored with respect to **10b**.



Scheme 6. Reaction pathway proposed for hydride insertion in **2b**. Relative energies of intermediates and energy barriers (in brackets) are included. All values calculated in benzene solvent [kcal/mol].

Scheme 7. Reaction pathways proposed for the formation of **6a** (II) and **10** (III).Figure 3. Energy profile of the reaction leading to complexes **6a** (II) and **10** (III), showing the pathway: (a) from the dissociation of **1** (**2a+2b**) either to product **6a** or to intermediate **7b**, by means of plain or discontinuous lines, respectively, and (b) from **3a+7b** to **10** by dotted lines.

Formation of the $[(dhpp)Pt(\mu-SC_4H_5-C,S)Pt(dhpp)]^+$ Cation (**10**)

Up to now the successive pathways leading to complexes **6a** and **7b** have been considered separately (Schemes 4, 5, and 6). In this subsection they will be assembled to enable the formation of **10**, model of the experimental complex **III**. The overall mechanism is summarized in Scheme 7, where the complexes described in the experimental section are highlighted within dashed-line squares. The energy profile for the sequence of reactions that take place after fragmentation of **I** to finally afford **6a** and **10** is depicted in Figure 3.

As shown in Scheme 7, fragmentation of the dinuclear platinum trihydride leads to **2a** and **2b**. At this point, these complexes react through different pathways. On the one hand, complex **2a** undergoes H_2 elimination to give **3a**, which subsequently reacts with thiophene to yield **6a** (II). On the other, the hydride migration to C2 in complex **2b**

(more favored than to C3) leads to **6b**. This intermediate is able to activate the C–S bond to give the very unstable **7b** complex. Reaction of the latter species with **3a** gives the dinuclear platinum complex **10** without energy barrier (Figure 3). The energy of this complex is 29.5 kcal/mol below that of **2a+2b** and, despite the unfavorable entropic contribution of the association process, the $2a+2b \rightarrow 10$ reaction is also favored on Gibbs energy grounds with $\Delta G_{\text{benzene}} = -20.8$ kcal/mol.

Calculations versus Experiments

All previous considerations account for the overall mechanism from **1** (I) to either **6a** (II) or **10** (III). The next step is to analyze their consistency with the experimental results. Thus, concerning the reaction of **I** with **I-d₃**, the formation of a mixture of isotopomers **I-d_x** ($x = 0-3$) was

experimentally observed only in the presence of thiophene at reflux temperature. This is consistent with the equilibrium between **1+T** and **2a+2b** depicted in Scheme 4. This reaction has an energy cost of 21.7 kcal/mol while the fragmentation of **I** without the presence of thiophene requires 39.5 kcal/mol. On the other hand, replacement of **I** by **I-d₃** in the synthesis of **III** showed that the hydrogen atom inserted into the thiophenic ring comes from **I** and adds to the C2 atom. This result fits well with the mechanism showed in Scheme 7, in which the formation of **10 (III)** involves an initial insertion of the hydride into the C2 position of the coordinated thiophene in **2b**.

The general mechanism proposed can also account for the noninterconversion between **II** and **III** even in the presence of external hydride ligands. Comparison of **II** and **III** indicates that this transformation would imply the hydride insertion into the thiophenic ring of **II** and the subsequent coordination of an additional {(dppp)Pt} fragment. On the basis of Scheme 7, two steps leading to **III** deserve special consideration. First, the intramolecular hydride migration in species **2b**, which entails a low energy barrier, and second, the stabilization of the intermediate **7b** by means of its coordination to a {(dppp)Pt} fragment. Remarkably, none of these two features can be accomplished in the experimental system. On the one hand, **II** does not enclose platinum-bound hydride ligands, thus hampering an intramolecular hydride migration. On the other, formation of **III** would require the assistance of the {(dppp)Pt} fragment, which only forms from the thiophene-promoted dissociation of **I**. Overall, theoretical results account for the fact that **II** does not evolve into **III**, even in the presence of **I** or NaBH₄.

Another experimental feature of the reaction of **I** with **T** refers to the different relative amounts of the reaction products, **II** and **III**, depending on the reaction conditions. Thus, the reaction affords **II (6a)** and **III (10)** in a 2:3 or 1:9 molar ratio using neat thiophene or organic solvent (toluene or benzene), respectively. The energy profile depicted in Figure 3 shows that the highest energies involved in the formation of **6a** and **10 (TS4: 34.2 kcal/mol and 3a+7b: 31.0 kcal/mol, respectively)** are very similar. Consequently, small changes in the reaction conditions can affect these energies, modifying the molar ratio of products. In addition, the concentration of thiophene also influences the **II** to **III** molar ratio because the two parallel pathways leading to **6a** and **10** involve a different number of thiophene molecules. The minor relative amount obtained for **II** in benzene or toluene can be explained considering that two molecules of **T** are required to form this complex, one to dissociate the starting complex **I** and the other to react with **3a** (see Scheme 7). Overall, the formation of **II** in toluene or benzene will be disfavored versus **III**, whose formation requires only one molecule of **T**.

Conclusions

C–S bond activation of thiophene (**T**) by the dinuclear trihydride platinum complex [(dppp)₂Pt₂H₃]ClO₄ (**I**) af-

forded the mononuclear [(dppp)Pt(SC₄H₄-C,S)] (**II**) metal-acycle that involves activation of the thiophenic C–S bond exclusively, and the dinuclear [(dppp)₂Pt₂(μ-SC₄H₅-C,S)ClO₄] (**III**) complex, where activation of this bond is concomitant with the partial hydrogenation of thiophene (Scheme 2).

Additional experiments and computational results have evidenced the role of **T** as promoter of the cleavage of **I** into the [(dppp)PtH₂] and [(dppp)PtH(C₄H₄S-κS)]⁺ fragments in the first step of the reaction. Also, experimental observations showing the noninterconversion equilibrium between **II/III** indicate that two concurrent mechanisms are at work. This is fully consistent with the theoretical calculations, which allow us to propose two different reaction pathways that originate after the dissociation of **I**. While formation of **II** involves exclusive participation of the former fragment, both are required to take part in the pathway leading to **III**. In fact, formation of this complex implies the coordination of {(dppp)Pt} to [(dppp)Pt(μ-SC₄H₅-C,S)]⁺ (Scheme 7). The former species, which originates from [(dppp)PtH₂], is responsible for the stabilization of the latter, which arises from the hydride migration into the thiophenic ring in [(dppp)PtH(C₄H₄S-κS)]⁺ and subsequent C–S bond activation. Remarkably, complex **III** is the first example of a platinum complex involving C–S bond activation and hydrogenation of thiophene.

The reactions of platinum complexes **II–V** with protonic acids and hydride sources have shown the ability of these reagents to give total desulfurization (Scheme 3). Thus, the reaction of **II** and **III** with protonic acids affords either partial hydrogenation of the thiophenic chain (with HBF₄) or formation of thiols (with HCl). On the other hand, the reaction with NaBH₄ entails the formation of H₂S only from complexes where the thiophenic chain has been partially hydrogenated (**III–V**). This result is consistent with the assumption that metal hydride complexes are keystones in the desulfurization of thiophene.

Overall, the combination of experimental and theoretical studies of the reaction of [(dppp)₂Pt₂H₃]ClO₄ with thiophene has provided new insights into the mechanism of the homogeneous HDS. Notwithstanding this progress, designing systems able to perform the reaction of completely and efficiently desulfurizing thiophene and in softer conditions still appears to be the main goal. The importance of this reaction makes any effort in this direction worthwhile.

Experimental Section

Materials and Methods: All reactions were carried out under pure dinitrogen, and conventionally dried and degassed solvents were used throughout. These were Purex Analytical Grade from SDS. Thiophene (≥99%) was purchased from Aldrich. It was purified following a reported procedure.^[70] Commercial 0.5 M NaMeO in methanol and NEt₃ (99%, *d* = 0.726 g/cm³) were used without further purification. The synthesis and spectroscopic characterization of [(dppp)₂Pt₂H₃]ClO₄ (**I**) and [(dppp)₂Pt₂D₃]ClO₄ (**I-d₃**) as well as the X-ray structure of **I** have already been reported.^[50] Elemental

analyses were performed on a Carlo–Erba CHNS EA-1108 analyzer. IR spectra were recorded with a Perkin–Elmer FT-2000 spectrophotometer using KBr pellets. ^1H , $^1\text{H}\{^{31}\text{P}\}$, ^{13}C DEPT, ^{31}P , $^{31}\text{P}\{^1\text{H}\}$, $^{31}\text{P}\text{-}^1\text{H}$ HMBC, ^{195}Pt , and $^{195}\text{Pt}\{^1\text{H}\}$ NMR and $^1\text{H}\text{-}^1\text{H}$ NOESY, $^1\text{H}\text{-}^1\text{H}$ COSY, $^{13}\text{C}\text{-}^1\text{H}$ HMQC, and $^{13}\text{C}\text{-}^1\text{H}$ HSQC-edit spectra were performed unless otherwise indicated from samples in solution at room temperature with a Bruker Avance DRX-360 spectrometer operating at 360.13 MHz for ^1H , 90.56 MHz for ^{13}C , 145.79 MHz for ^{31}P , and 77.42 MHz for ^{195}Pt . ^1H and ^{13}C chemical shifts are relative to SiMe_4 , ^{31}P to external 85% H_3PO_4 , and ^{195}Pt to external 1 M $\text{Na}_2[\text{PtCl}_6]$ in D_2O . The $^{31}\text{P}\{^1\text{H}\}$ NMR spectrum of **III** was simulated on a Pentium[®]-200 computer using the gNMR V4.0.1 program.^[71] ^2H NMR experiments were performed from samples in $\text{CDCl}_3/\text{CHCl}_3$ mixture solutions at room temperature with a Bruker Avance-500 operating at 76.75 MHz. ^2H NMR chemical shifts are relative to CDCl_3 . ^{19}F NMR experiments for **IV** and **V** were performed from samples in acetone solutions at room temperature with a Bruker DPX-250 operating at 235.33 MHz. ^{19}F NMR chemical shifts are relative to CFCl_3 . H and C labels for complexes **III–V** are shown in Figure 4.

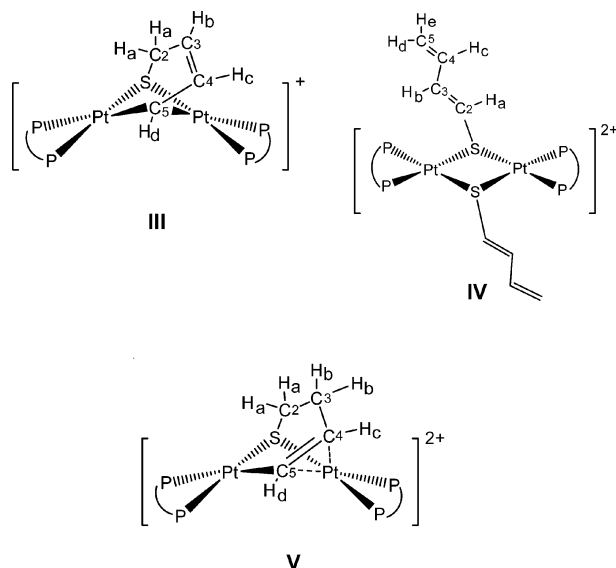


Figure 4. H and C labels for complexes **III–V**.

The ESI-MS measurements were performed on a VG Quattro Micromass Instrument under already described experimental conditions.^[50] The carrier was a 1:1 mixture of acetonitrile and water containing formic acid (1–10%). The exact mass for **III** was determined on a microTOF-Q instrument using direct injection from HPLC 1200RR and Apollo II ESI ionization source. GC-MS spectra were recorded using a Hewlett–Packard 6890 instrument and a Hewlett–Packard 5973 electronic impact mass detector.

Caution: Although no problems were encountered in this work, all perchlorate compounds are potentially explosive, and should be handled in small quantities and with great care!

Synthesis of [(dppp)Pt(SC₄H₄-C,S)] (II): The white-beige suspension formed by addition of **I** (200 mg, 0.15 mmol) to degassed neat thiophene (15 mL) was heated at reflux temperature (100 °C) for 24 h, by which time it had turned into a red-brown solution containing a minor amount of a black solid residue. This was separated by filtration through Celite and the remaining solution evaporated under vacuum to yield a brown residue. This solid was dissolved in

toluene and the solution chromatographed on a neutral alumina column. Elution with a hexane/benzene mixture at 20% ratio showed separation of two bands, yellow and red-brown, which respectively contained complexes **II** and **III**. Extraction of the former band followed by removal of the solvent under vacuum produced a residue that was dissolved in acetone and precipitated with diethyl ether. The yellow solid thus formed was collected by filtration, washed with diethyl ether, and vacuum dried. Yield 52 mg, 25%. ^1H NMR (360 MHz, CDCl_3 , 25 °C): δ = 6.75 (t, 1 H, CH), 6.92 (1 H, CH), 7.18 (1 H, CH), 7.34 (1 H, CH) ppm. ^{13}C DEPT NMR (91 MHz, CDCl_3 , 25 °C): δ = 119.1 (CH), 120.8 (CH), 124.4 (CH), 130.2 (CH) ppm. $^{31}\text{P}\{^1\text{H}\}$ NMR (146 MHz, CDCl_3 , 25 °C): δ = 6.56 (d, $^1J_{\text{Pt,P}} = 3064.4$, $^2J_{\text{P,P}} = 33.0$ Hz), -1.10 (d, $^1J_{\text{Pt,P}} = 1601.8$, $^2J_{\text{P,P}} = 33.0$ Hz) ppm. ^{195}Pt NMR (77 MHz, CDCl_3 , 25 °C): δ = -4525 (dd, $^1J_{\text{P,Pt}} = 3066$ and 1605 Hz) ppm. ESI-MS: $m/z = 692.2$ [$\text{M} + 1$]⁺. $\text{C}_{31}\text{H}_{30}\text{P}_2\text{S}$ (691.2): calcd. C 53.83, H 4.37, S 4.64; found C 53.95, H 4.29, S 4.75. Attempts to obtain crystals suitable for X-ray diffraction were unsuccessful.

Synthesis of [(dppp)₂Pt₂(μ-SC₄H₅-C,S)]ClO₄ (III): The same reaction procedure as for **II** but in the presence of toluene or benzene led essentially to **III**. Thus, **I** (200 mg, 0.15 mmol) and neat thiophene (15 mL) were made to react in degassed toluene or benzene (20 mL). Column chromatography under the same experimental conditions as above allowed elution of the second red-brown band with benzene. Removal of the solvent under vacuum produced a residue that was dissolved in acetone and precipitated with diethyl ether. The precipitated yellow-brown solid was collected by filtration, washed with diethyl ether, and vacuum dried. Yield 83 mg, 43%. ^1H NMR (360 MHz, $[\text{D}_6]\text{acetone}$, 25 °C): δ = 1.62 (br., 2 H_a), 2.77 (br., H_d), 5.36 (dt, $^3J_{\text{Hb,Hc}} = 3.6$, $^3J_{\text{Hb,Hc}} = 9.4$ Hz, H_b), 5.46 (dt, $^3J_{\text{Hc,Hb}} = 9.4$, $^3J_{\text{Hc,Hd}} = 8.2$ Hz, H_c) ppm. ^{13}C DEPT NMR (91 MHz, $[\text{D}_6]\text{acetone}$, 25 °C): δ = 33.0 (C2), 42.7 (C5), 126.1 (C3), 137.1 (C4) ppm. $^{31}\text{P}\{^1\text{H}\}$ NMR (146 MHz, $[\text{D}_6]\text{acetone}$, 25 °C): δ = 3.02 (d, $^1J_{\text{Pt,P}} = 3869.6$ Hz), 1.96 ($^1J_{\text{Pt,P}} = 1857.0$ Hz) ppm. On the basis of the simulation of the $^{31}\text{P}\{^1\text{H}\}$ NMR spectrum including long-range P–P and P–Pt couplings: $^3J_{\text{P',P'}} = 22.0$, $^3J_{\text{P',P''}} = 4.7$, and $^2J_{\text{P',P''}} = -22.3$ Hz, where P' and P'' are nonequivalent phosphorus nuclei, and $^2J_{\text{P,Pt}} = 56$ Hz ($\delta_{\text{P}} = 1.96$ ppm) and 37 Hz ($\delta_{\text{P}} = 3.02$ ppm). $^{195}\text{Pt}\{^1\text{H}\}$ NMR (77 MHz, $[\text{D}_6]\text{acetone}$, 25 °C): δ = -4670 (dd, $^1J_{\text{P,Pt}} = 3872$ and 1867 Hz) ppm. ESI-MS: $m/z = 1299.2401$ [$\text{M} - \text{ClO}_4$]⁺. $\text{C}_{58}\text{H}_{57}\text{ClO}_4\text{P}_4\text{Pt}_2\text{S}$ (1399.64): calcd. C 49.77, H 4.10, S 2.29; found C 49.02, H 3.82, S 2.11. IR (cm^{-1}): $\tilde{\nu} = 1094$ i, br. (ClO_4). Attempts to obtain crystals suitable for X-ray diffraction were unsuccessful.

Replacement of **I** by **I-d₃** in the above reaction procedure allowed unequivocal identification of [(dppp)₂Pt₂(μ-SC₄H₄D-C,S)]⁺ (**III-d₁**) on the basis of NMR spectroscopic data. ^1H NMR (360 MHz, $[\text{D}_6]\text{acetone}$, 25 °C): δ = 1.63 (br., H_a), 2.77 (br., H_d), 5.36 (br., H_b), 5.46 (br., H_c) ppm. ^2H NMR (77 MHz, $\text{CDCl}_3/\text{CHCl}_3$, 25 °C): δ = 1.58 (br., D_a) ppm. ^{13}C -DEPT NMR (91 MHz, $[\text{D}_6]\text{acetone}$, 25 °C): δ = 32.6 (C2), 42.7 (C5), 126.1 (C3), 137.1 (C4) ppm. NMR features corresponding to the dppp terminal ligands were coincident with those of **III**.

Synthesis of [(dppp)₂Pt₂(μ-SC₄H₅)₂](BF₄)₂ (IV): Aqueous HBF₄ (70 μL of 4 M solution, 0.28 mmol) was added to a solution of **II** (50 mg, 0.07 mmol) in CH_3CN (10 mL). The mixture was stirred (15 min) and then evaporated to 5 mL under vacuum. Addition of diethyl ether gave a white precipitate, which was dissolved in ethyl acetate and purified on a neutral alumina column using the same solvent as eluent. Evaporation of the solvent afforded a white solid. Yield 47 mg, 84%. ^1H NMR (360 MHz, CD_3CN , 25 °C): δ = 4.75 (d, $^3J_{\text{Ha,Hc}} = 10$, $^2J_{\text{Ha,Hb}} < 1$ Hz, H_a), 4.90 (d, $^3J_{\text{Hb,Hc}} = 16.5$ Hz,

H_b), 5.34 (dt, $^3J_{\text{Hc,Ha}} = ^3J_{\text{Hc,Hd}} = 10$, $^3J_{\text{Hc,Hb}} = 16$ Hz, H_c), 5.45 (d, $^3J_{\text{He,Hd}} = 10$ Hz, H_e), 5.74 (t, $^3J_{\text{Hd,He}} = ^3J_{\text{Hd,Hc}} = 10$ Hz, H_d) ppm. ^{13}C DEPT NMR (91 MHz, CD₃CN, 25 °C): $\delta = 136.6$ (C₄), 127.4 (C₃), 120.8 (C₂), 117.4 (C₅) ppm. $^{31}\text{P}\{^1\text{H}\}$ NMR (146 MHz, CD₃CN, 25 °C): $\delta = -2.00$ ($^1J_{\text{Pt,P}} = 2897.4$ Hz) ppm. ^{19}F NMR (235 MHz, [D₆]acetone, 25 °C): $\delta = -152.2$ ppm. $^{195}\text{Pt}\{^1\text{H}\}$ NMR (77 MHz, CD₃CN, -20 °C): $\delta = -4415.8$ ppm. C₆₂H₆₂B₂F₈P₄Pt₂S₂ (1558.94): calcd. C 47.77, H 4.01, S 4.11; found C 47.96, H 4.16, S 4.27. ESI MS (*m/z*): 693.5 (25%) corresponding to [(dppp)₂Pt₂(SC₄H₅)₂]²⁺, and 1387.0 (100%) corresponding to [(dppp)₂Pt₂(SC₄H₅)₂]⁺. IR: $\tilde{\nu} = 1051$ i, br. (BF₄).

Synthesis of [(dppp)₂Pt₂(μ-SC₄H₆)](BF₄)₂ (V): Aqueous HBF₄ (50 μL of 4 M solution, 0.20 mmol) was added to a solution of III (75 mg, 0.05 mmol) in degassed acetonitrile (10 mL) and the mixture stirred for 30 min. Then it was filtered through Celite, concentrated to 1–2 mL, and precipitated with addition of diethyl ether to yield a yellow solid. The solid was collected by filtration, washed with diethyl ether, and vacuum dried. Yield 65 mg, 82%. ^1H NMR (360 MHz, [D₆]acetone, 25 °C): $\delta = 2.67$ (br., 2H_b), 2.78 (br., 2H_a), 5.31 (dt, $^3J_{\text{Hc,Hb}} = 3.2$, $^3J_{\text{Hc,Hd}} = 9.2$ Hz, H_c), 5.90 (d, $^3J_{\text{Hd,Hc}} = 9.2$ Hz, H_d) ppm. ^{13}C DEPT NMR (91 MHz, [D₆]acetone, 25 °C): $\delta = 26.8$ (C₂), 33.3 (C₃), 119.7 (C₅), 129.7 (C₄) ppm. $^{31}\text{P}\{^1\text{H}\}$ NMR (146 MHz, [D₆]acetone, 25 °C): $\delta = 0.10$ (d, $^1J_{\text{Pt,P}} = 2612.4$ Hz), -0.92 ($^1J_{\text{Pt,P}} = 2965.3$ Hz) ppm. $^{195}\text{Pt}\{^1\text{H}\}$ NMR (77 MHz, [D₆]acetone, 25 °C): $\delta = -4675$ (dd, $^1J_{\text{Pt,Pt}} = 2612$ and 2966 Hz) ppm. ^{19}F NMR (235 MHz, [D₆]acetone, 25 °C): $\delta = -152.2$ ppm. ESI-MS: *m/z* = 650.3 (15%) and 1300.3 (100%) corresponding to [(dppp)₂Pt₂(SC₄H₆)₂]²⁺ and [(dppp)₂Pt₂(SC₄H₆)₂]⁺, respectively. C₅₈H₅₈B₂F₈P₄Pt₂S (1474.80): calcd. C 47.23, H 3.96, S 2.17; found C 47.14, H 4.01, S 2.12. IR: $\tilde{\nu} = 1051$ i, br. (BF₄).

The same reaction procedure but using only 1.2 equiv. of HBF₄ allowed separation of a yellow solid, whose acetone solution afforded adequate crystals for X-ray diffraction.

Reaction of V with Bases (NaOMe, Et₃N): A methanol solution of NaOMe (100 μL, 0.05 mmol) or Et₃N (17.5 μL, 0.125 mmol) was added to a suspension of V (75 mg, 0.05 mmol) in CH₃CN (10 mL). In both cases the resulting solution was stirred at room temperature for 30 min, after which time it was concentrated to dryness. Then, the solid was redissolved in benzene, filtered and precipitated by addition of diethyl ether. ^1H and ^{31}P NMR spectroscopic data of this solid in acetone solution evidenced the complete transformation of V into III.

Reaction of II–V with HCl: An excess of HCl was added to separate stirred CH₂Cl₂ (10 mL) solutions containing II, III, IV, or V (25 mg) in a 3–4:1 molar ratio at room temperature. The initial yellow-brown solution turned pale yellow and a white solid precipitated. After 30 min of stirring, the mixture was filtered and the soluble part analyzed by CG-MS. The solid was unequivocally identified as [(dppp)PtCl₂] (65–80% yield) by NMR spectroscopy.^[72,73] The solution was shown to be composed mainly of thiophene in the case of II, thiapentadiene or an isomer thereof (C₄H₆S) and thiophene^[52] in a 4:1 molar ratio for IV, and a mixture of HS–CH₂–CH=CH–CH₃^[74] and HS–CH₂–CH₂–CH=CH₂^[47] in 4:1 and 1:1 molar ratios, for III and V, respectively.

Reaction of II–V with NaBH₄: Solid NaBH₄ was made to react with separate stirred THF/EtOH_{abs} solutions (10 mL) containing II, III, IV, or V (25 mg) in a 4:1 molar ratio at room temperature under a closed atmosphere. In the reactions involving III–V, formation of a black precipitate of Ag₂S on a filter paper soaked with silver nitrate gave evidence of formation of H₂S. In all cases, after 20 h of stirring the initial yellow-brown solution became a dark-brown suspension. The black solid was separated and the solution ana-

lyzed by CG-MS. The solution was shown to contain thiophene in the case of II, but no thiols and/or organic volatiles were detected.

X-ray Crystallographic Characterization: A summary of crystal data, data collection, and refinement parameters for the structural analysis of complex [(dppp)Pt(μ-SC₄H₆)Pt(dppp)]₂(BF₄)_{2.95}(ClO₄)_{1.05} is given in Table 3. Measurements of diffraction intensity data were collected on a Bruker SMART CCD-1000 area-detector diffractometer with graphite-monochromated Mo-*K*_α radiation ($\lambda = 0.71073$ Å). During the initial unit cell determination it was recognized that the crystal was twinned. Several crystals were assayed but all possessed the same diffraction pattern, so a small but diffracting crystal was chosen. The collected reflections were processed with the program CELLNOW^[75] which established two twin components with a ratio of 0.72/0.28. In order to process the twinned data, the absorption correction was applied using the multiscan TWINABS^[75] program. Cell parameters were obtained from least-squares fit on the observed setting angles of all significant intensity reflections. A Patterson map solution of the structure to locate platinum atoms, followed by expansion of the structure with the program DIRDIF^[76] revealed all non-hydrogen atoms. The structure was resolved by direct methods and refined by full-matrix least-squares based on *F*², with the aid of SHELX-97^[77] software. The thiolate ligand was modeled as two disordered SCH₂CH₂CH=CH moieties with opposite orientations, finding a refined population ratio of 63/37 in one dinuclear complex and 69/31 in the other. All non-hydrogen atoms were anisotropically refined. All hydrogen atoms were included at geometrically calculated positions with thermal parameters derived from the parent atoms. Molecular graphics are represented by ORTEP-3 for Windows.

Table 3. Crystallographic data for [(dppp)Pt(μ-SC₄H₆)Pt(dppp)]₂(BF₄)_{2.95}(ClO₄)_{1.05}.

Empirical formula	2(C ₅₈ H ₅₆ P ₄ Pt ₂ S)·2.95(BF ₄)·1.05(ClO ₄)·3(C ₃ H ₆ O)·(H ₂ O)
<i>M</i>	3153.06
Crystal system	monoclinic
Space group	<i>Cc</i>
<i>a</i> [Å]	43.8827(12)
<i>b</i> [Å]	14.1377(4)
<i>c</i> [Å]	22.2630(6)
α [°]	90
β [°]	116.223(1)
γ [°]	90
<i>V</i> [Å ³]	12390.5(6)
<i>T</i> [K]	100.0(1)
<i>Z</i>	4
<i>D</i> _{calcd} [g/cm ³]	1.690
μ [mm ⁻¹]	4.735
Reflections collected/unique reflections/ <i>R</i> _{int}	222291/45071/0.0826
Parameters/restraints	1289/68
Goodness-of-fit on <i>F</i> ²	0.926
Twin law	twofold axis along <i>c</i> *
Twin domain populations	0.720(4)/0.280(4)
Absolute structure parameter	0.000(4)
<i>R</i> ₁ , <i>wR</i> ₂ [<i>I</i> > 2σ(<i>I</i>)]	0.0437, 0.0970
<i>R</i> ₁ , <i>wR</i> ₂ (all data)	0.0776, 0.1056
Largest diff. peak, hole [e/Å ³]	1.228, -1.130

CCDC-651579 {compound [(dppp)Pt(μ-SC₄H₆)Pt(dppp)]₂(BF₄)_{2.95}(ClO₄)_{1.05}} contains the supplementary crystallographic data for this paper. These data can be obtained free of charge from The Cambridge Crystallographic Data Centre via www.ccdc.cam.ac.uk/data_request/cif.

Computational Details: The calculations were performed with the Gaussian03 package,^[78] using Density Functional Theory with the B3LYP functional.^[79–81] For the Pt, P, and S atoms, the lan12dz effective core potential was used to describe the inner electrons,^[78,82,83] whereas their associated double- ζ basis set was employed for the remaining electrons. An extra series of d-polarization functions was also added for P (exp. 0.387) and S (exp. 0.503).^[84] The three hydrides and the carbon atoms of thiophene were described by the 6-31G(d,p) basis set^[85] and the remaining C and H atoms were described by the 6-31G basis set. The structures of the reactants, intermediates, transition states, and products were fully optimized in gas phase without any symmetry restriction. Frequency calculations were performed on all optimized structures, using the B3LYP functional, to characterize the stationary points as minima or TSs, as well as for the calculation of gas-phase Gibbs energies (G) at 298 K. Single-point solvent calculations were performed at optimized gas-phase geometries, using the CPCM approach,^[86,87] which is an implementation of the conductor-like screening solvation model (COSMO) in Gaussian03.^[88] Benzene, the solvent used in some experiments, was chosen as solvent (dielectric constant $\epsilon = 2.247$). In this way $\Delta E_{\text{benzene}}$, resulting from adding the contribution of the Gibbs energy of solvation to the gas phase internal energies, were obtained.

Supporting Information (see also the footnote on the first page of this article): Comparison of the $^{31}\text{P}\{^1\text{H}\}$ NMR spectrum of **III** with its computed simulation. Table includes total energies and Cartesian coordinates of the optimized structures reported in the text.

Acknowledgments

Financial support from the Spanish Ministerio de Educación y Ciencia (MEC) through Projects CTQ2004-01463 and CTQ2005-09000-C02-01 and from the Generalitat de Catalunya (GENCAT) through grant 2005SGR00896 is gratefully acknowledged. A. L. is indebted to GENCAT for a “Distinció per a la Promoció de la Recerca Universitària”. We are grateful to Dr. T. Parella and Dr. J. Sola (UAB) for interesting discussions on NMR spectroscopic data, and to Dr. A. L. Llamas and Dr. B. Dacuña of the USC for crystal structure determination.

- [1] R. J. Angelici, *Acc. Chem. Res.* **1988**, *21*, 387–394.
- [2] C. Bianchini, A. Meli, *J. Chem. Soc. Dalton Trans.* **1996**, 801–814.
- [3] C. Bianchini, A. Meli in *Applied Homogeneous Catalysis with Organometallic Compounds* (Eds.: B. Cornils, W. A. Herrmann), VCH, Weinheim, Germany, **1996**, vol. 2, p. 969.
- [4] W. D. Jones, D. A. Vacic, R. M. Chin, J. H. Roache, A. W. Myers, *Polyhedron* **1997**, *16*, 3115–3128.
- [5] R. J. Angelici, *Polyhedron* **1997**, *16*, 3073–3088.
- [6] R. A. Sánchez-Delgado, *Organometallic Modeling of the Hydrodesulfurization and Hydrodenitrogenation Reactions*, Kluwer Academic Publishers, Dordrecht, **2002**.
- [7] R. R. Chianelli, M. Daage, M. J. Ledoux, *Adv. Catal.* **1994**, *40*, 177–232.
- [8] C. N. Satterfield, *Heterogeneous Catalysis in Industrial Practice*, McGraw-Hill, New York, **1991**.
- [9] D. Stirling, *The Sulfur Problem: Cleaning Up Industrial Feedstocks*, RSC Clean Technology Monographs (Ed.: J. H. Clark), The Royal Society of Chemistry, Cambridge, U.K., **2000**.
- [10] H. Topsøe, B. S. Clausen, F. E. Massoth, *Hydrotreating Catalysis*, Springer Berlin, **1996**, vol. 11.
- [11] A. N. Startsev, *Cat. Rev. - Sci. Eng.* **1995**, *37*, 353–423.
- [12] R. Navarro, B. Pawelec, J. L. G. Fierro, P. T. Vasudevan, J. F. Cambra, P. L. Arias, *Appl. Catal., A* **1996**, *137*, 269–286.
- [13] P. T. Vasudevan, J. L. G. Fierro, *Cat. Rev. - Sci. Eng.* **1996**, *38*, 161–188.
- [14] R. Prins, V. H. J. Debeer, G. A. Somorjai, *Cat. Rev. - Sci. Eng.* **1989**, *31*, 1–41.
- [15] C. M. Friend, J. T. Roberts, *Acc. Chem. Res.* **1988**, *21*, 394–400.
- [16] C. Bianchini, A. Meli, *Acc. Chem. Res.* **1998**, *31*, 109–116.
- [17] R. J. Angelici, *Organometallics* **2001**, *20*, 1259–1275.
- [18] T. B. Rauchfuss, *Prog. Inorg. Chem.* **1991**, *39*, 259–329.
- [19] X. Q. Yao, Y. W. Li, H. J. Jiao, *J. Mol. Struct.* **2005**, *726*, 67–80.
- [20] X. Q. Yao, Y. W. Li, H. J. Jiao, *J. Mol. Struct.* **2005**, *726*, 81–92.
- [21] S. Cristol, J. F. Paul, C. Schovsbo, E. Veilly, E. Payen, *J. Catal.* **2006**, *239*, 145–153.
- [22] R. R. Chianelli, G. Berhault, P. Raybaud, S. Kasztelan, J. Hafner, H. Toulhoat, *Appl. Catal., A* **2002**, *227*, 83–96.
- [23] P. Raybaud, J. Hafner, G. Kresse, H. Toulhoat, *Phys. Rev. Lett.* **1998**, *80*, 1481–1484.
- [24] J. B. Chen, R. J. Angelici, *Coord. Chem. Rev.* **2000**, *206*, 63–99.
- [25] M. D. Curtis, S. H. Druker, *J. Am. Chem. Soc.* **1997**, *119*, 1027–1036.
- [26] U. Riaz, O. J. Curnow, M. D. Curtis, *J. Am. Chem. Soc.* **1994**, *116*, 4357–4363.
- [27] R. J. Angelici in *Encyclopedia of Inorganic Chemistry* (Ed.: R. B. King), John Wiley & Sons, New York, **1994**, vol. 3, pp. 1433–1443.
- [28] M. J. Ledoux, O. Michaux, G. Agostini, P. Panissod, *J. Catal.* **1986**, *102*, 275–288.
- [29] J. P. R. Vissers, C. K. Groot, E. M. Vanoers, V. H. J. Debeer, R. Prins, *Bull. Soc. Chim. Belg.* **1984**, *93*, 813–821.
- [30] T. A. Pecoraro, R. R. Chianelli, *J. Catal.* **1981**, *67*, 430–445.
- [31] D. G. Churchill, B. M. Bridgewater, G. Parkin, *J. Am. Chem. Soc.* **2000**, *122*, 178–179.
- [32] D. A. Vacic, W. D. Jones, *Organometallics* **1997**, *16*, 1912–1919.
- [33] D. A. Vacic, W. D. Jones, *J. Am. Chem. Soc.* **1999**, *121*, 7606–7617.
- [34] W. D. Jones, L. Z. Dong, *J. Am. Chem. Soc.* **1991**, *113*, 559–564.
- [35] J. J. García, B. E. Mann, H. Adams, N. A. Bailey, P. M. Maitlis, *J. Am. Chem. Soc.* **1995**, *117*, 2179–2186.
- [36] T. A. Atesin, S. S. Oster, K. Skugrud, W. D. Jones, *Inorg. Chim. Acta* **2006**, *359*, 2798–2805.
- [37] H. E. Selnau, J. S. Merola, *Organometallics* **1993**, *12*, 1583–1591.
- [38] W. D. Jones, R. M. Chin, T. W. Crane, D. M. Baruch, *Organometallics* **1994**, *13*, 4448–4452.
- [39] R. M. Chin, W. D. Jones, *Angew. Chem. Int. Ed. Engl.* **1992**, *31*, 357–358.
- [40] W. D. Jones, R. M. Chin, C. L. Hoaglin, *Organometallics* **1999**, *18*, 1786–1790.
- [41] W. D. Jones, R. M. Chin, *Organometallics* **1992**, *11*, 2698–2700.
- [42] L. Z. Dong, S. B. Duckett, K. F. Ohman, W. D. Jones, *J. Am. Chem. Soc.* **1992**, *114*, 151–160.
- [43] A. L. Sargent, E. P. Titus, *Organometallics* **1998**, *17*, 65–77.
- [44] O. Maresca, F. Maseras, A. Lledós, *New J. Chem.* **2004**, *28*, 625–630.
- [45] W. D. Jones, R. M. Chin, *J. Am. Chem. Soc.* **1994**, *116*, 198–203.
- [46] K. E. Janak, J. M. Tanski, D. G. Churchill, G. Parkin, *J. Am. Chem. Soc.* **2002**, *124*, 4182–4183.
- [47] C. Bianchini, A. Meli, M. Peruzzini, F. Vizza, P. Frediani, V. Herrera, R. A. Sánchez-Delgado, *J. Am. Chem. Soc.* **1993**, *115*, 2731–2742.
- [48] R. Navarro, B. Pawelec, J. L. G. Fierro, P. T. Vasudevan, *Appl. Catal., A* **1996**, *148*, 23–40.
- [49] Y. Kanda, T. Kobayashi, Y. Uemichi, S. Namba, M. Sugioka, *Appl. Catal., A* **2006**, *308*, 111–118.

- [50] F. Novio, P. González-Duarte, A. Lledós, R. Mas-Ballesté, *Chem. Eur. J.* **2007**, *13*, 1047–1063.
- [51] C. Bianchini, A. Meli, M. Peruzzini, F. Vizza, V. Herrera, R. A. Sanchez-Delgado, *Organometallics* **1994**, *13*, 721–730.
- [52] J. J. García, A. Arévalo, V. Montiel, F. Del Río, B. Quiroz, H. Adams, P. M. Maitlis, *Organometallics* **1997**, *16*, 3216–3220.
- [53] While various attempts to obtain single crystals of **V** were unsuccessful, recrystallization in acetone of the compound obtained by the reaction of **III** with HBF_4 at a 1:1.2 molar ratio afforded suitable crystals for X-ray diffraction. These consisted of the cation of **V**, as evidenced by NMR spectroscopic data, and a mixture of BF_4^- and ClO_4^- counterions.
- [54] V. C. M. Smith, R. T. Aplin, J. M. Brown, M. B. Hursthouse, A. I. Karalulov, K. M. A. Malik, N. A. Cooley, *J. Am. Chem. Soc.* **1994**, *116*, 5180–5189.
- [55] P. González-Duarte, A. Lledós, R. Mas-Ballesté, *Eur. J. Inorg. Chem.* **2004**, 3585–3599.
- [56] G. Ujaque, F. Maseras in *Principles and Applications of Density Functional Theory in Inorganic Chemistry I*, Series: Structure and Bonding (Eds.: N. Kaltsoyannis, J. E. McGrady), Springer, Heidelberg, **2004**, vol. 112, pp. 117–150.
- [57] F. Maseras, A. Lledós, *Computational Modeling of Homogeneous Catalysis*, Kluwer Academic Publishers, Dordrecht, Boston, London, vol. 25, **2002**.
- [58] M. Palmer, K. Carter, S. Harris, *Organometallics* **1997**, *16*, 2448–2459.
- [59] C. Blonski, A. W. Myers, M. Palmer, S. Harris, W. D. Jones, *Organometallics* **1997**, *16*, 3819–3827.
- [60] S. Harris, *Polyhedron* **1997**, *16*, 3219–3233.
- [61] L. Rincon, J. Terra, D. Guenzburger, R. A. Sánchez-Delgado, *Organometallics* **1995**, *14*, 1292–1296.
- [62] S. Harris, *Organometallics* **1994**, *13*, 2628–2640.
- [63] H. Z. Li, K. Q. Yu, E. J. Watson, K. L. Virkaitis, J. S. D'Accholi, G. B. Carpenter, D. A. Sweigart, P. T. Czech, K. R. Overly, F. Coughlin, *Organometallics* **2002**, *21*, 1262–1270.
- [64] R. A. Sánchez-Delgado, V. Herrera, L. Rincón, A. Andriollo, G. Martin, *Organometallics* **1994**, *13*, 553–561.
- [65] A. L. Bandini, G. Banditelli, M. Manassero, A. Albinati, D. Colognesi, J. Eckert, *Eur. J. Inorg. Chem.* **2003**, 3958–3964.
- [66] T. Yoshida, T. Yamagata, T. H. Tulip, J. A. Ibers, S. Otsuka, *J. Am. Chem. Soc.* **1978**, *100*, 2063–2073.
- [67] D. J. Schwartz, R. A. Andersen, *J. Am. Chem. Soc.* **1995**, *117*, 4014–4025.
- [68] T. Matsubara, F. Maseras, N. Koga, K. Morokuma, *J. Phys. Chem.* **1996**, *100*, 2573–2580.
- [69] J. J. Low, W. A. Goddard, *Organometallics* **1986**, *5*, 609–622.
- [70] G. H. Spies, R. J. Angelici, *Organometallics* **1987**, *6*, 1897–1903.
- [71] P. H. M. Budzelaar, *gNMR*, v. 4.01, Cherwell Scientific Publishing Ltd., Oxford, U.K., **1997**.
- [72] M. P. Brown, R. J. Puddephatt, M. Rashidi, K. R. Seddon, *J. Chem. Soc. Dalton Trans.* **1977**, 951–955.
- [73] R. Mas-Ballesté, G. Aullón, P. A. Champkin, W. Clegg, C. Mégret, P. González-Duarte, A. Lledós, *Chem. Eur. J.* **2003**, *9*, 5023–5035.
- [74] W. F. Wood, B. G. Sollers, G. A. Dragoo, J. W. Dragoo, *J. Chem. Ecol.* **2002**, *28*, 1865–1870.
- [75] G. M. Sheldrick, *CELLNOW*, University of Göttingen, Germany, **2005**.
- [76] P. T. Beurskens, G. Admiraal, G. Beurskens, W. P. Bosman, R. de Gelder, R. Israel, J. M. Smits, *DIRDIF*, University of Nijmegen, The Netherlands, **1999**.
- [77] G. M. Sheldrick, *SHELX-97*, University of Göttingen, Germany, **1998**.
- [78] M. J. Frisch, G. W. Trucks, H. B. Schlegel, G. E. Scuseria, M. A. Robb, J. R. Cheeseman, J. A. J. Montgomery, T. Vreven, K. N. Kudin, J. C. Burant, J. M. Millam, S. S. Iyengar, J. Tomasi, V. Barone, B. Mennucci, M. Cossi, G. Scalmani, N. Rega, G. A. Petersson, H. Nakatsuji, M. Hada, M. Ehara, K. Toyota, R. Fukuda, J. Hasegawa, M. Ishida, T. Nakajima, Y. Honda, O. Kitao, H. Nakai, M. Klene, X. Li, J. E. Knox, H. P. Hratchian, J. B. Cross, C. Adamo, J. Jaramillo, R. Gomperts, R. E. Stratmann, O. Yazyev, A. J. Austin, R. Cammi, C. Pomelli, J. W. Ochterski, P. Y. Ayala, K. Morokuma, G. A. Voth, P. Salvador, J. J. Dannenberg, V. G. Zakrzewski, S. Dapprich, A. D. Daniels, M. C. Strain, O. Farkas, D. K. Malick, A. D. Rabuck, K. Raghavachari, J. B. Foresman, J. V. Ortiz, Q. Cui, A. G. Baboul, S. Clifford, J. Cioslowski, B. B. Stefanov, G. Liu, A. Liashenko, P. Piskorz, I. Komaromi, R. L. Martin, D. J. Fox, T. Keith, M. A. Al-Laham, C. Y. Peng, A. Nanayakkara, M. Challacombe, P. M. W. Gill, B. Johnson, W. Chen, M. W. Wong, C. Gonzalez, J. A. Pople, *Gaussian 03*, Revision C.02, Inc., Wallingford, CT, **2004**.
- [79] C. Lee, R. G. Parr, W. Yang, *Phys. Rev.* **1988**, *37*, B785.
- [80] A. D. Becke, *J. Chem. Phys.* **1993**, *98*, 5648–5652.
- [81] P. J. Stephens, F. J. Devlin, C. F. Chabalowski, M. J. Frisch, *J. Phys. Chem.* **1994**, *98*, 11623–11627.
- [82] P. J. Hay, W. R. Wadt, *J. Phys. Chem.* **1985**, *82*, 299–310.
- [83] W. R. Wadt, P. J. Hay, *J. Chem. Phys.* **1985**, *82*, 284–299.
- [84] A. Höllwarth, M. Böhme, S. Dapprich, A. W. Ehlers, A. Gobbi, V. Jonas, K. F. Köhler, R. Stegmann, A. Veldkamp, G. Frenking, *Chem. Phys. Lett.* **1993**, *208*, 237–240.
- [85] W. J. Hehre, R. Ditchfield, J. A. Pople, *J. Chem. Phys. A* **1972**, *56*, 2257–2261.
- [86] V. Barone, M. Cossi, *J. Phys. Chem. A* **1998**, *102*, 1995–2001.
- [87] M. Cossi, N. Rega, G. Scalmani, V. Barone, *J. Comput. Chem.* **2003**, *24*, 669–691.
- [88] J. Tomasi, M. Persico, *Chem. Rev.* **1994**, *94*, 2027–2094.

Received: September 7, 2007
Published Online: November 2, 2007